"ATTACHMENT A"

J|A|C|S
ARTICLES
Published on Web 09/24/2002

Mesostructured γ-Al_2O_3 with a Lathlike Framework Morphology

Zhaorong Zhang and Thomas J. Pinnavaia*

Contribution from the Department of Chemistry and Center for Fundamental Material Research, Michigan State University, East Lansing, Michigan 48824-1322

Received June 11, 2002

Abstract: A novel three-step assembly pathway is reported for the formation of a mesostructured alumina with framework pore walls made of crystalline, lathlike γ-Al_2O_3 nanoparticles. In the initial supramolecular assembly step of the pathway a mesostructured alumina with a wormhole framework morphology and amorphous pore walls is assembled through the hydrolysis of Al_{13} oligocations and hydrated aluminum cations in the presence of a nonionic diblock or triblock poly(ethylene oxide) surfactant as the structure-directing porogen. The walls of the initial mesostructure are then transformed in a second hydrolysis step at a higher temperature to a surfactant−boehmite mesophase, denoted MSU-S/B, with a lathlike framework made of boehmite nanoparticles. A final thermal reaction step topochemically converts the intermediate boehmitic mesophase to a mesostructure with crystalline γ-Al_2O_3 pore walls, denoted MSU-γ, with retention of the lathlike framework morphology. The boehmitic MSU-S/B intermediates formed from the chloride salts of aluminum incorporate chloride anions into the mesostructure. Chloride ion incorporation tends to disorder the nanoparticle assembly process, leading to a broadening of the slit-shaped framework pores in the final MSU-γ phases and to the introduction of intra- and interparticle textural mesopores. However, the well-ordered MSU-γ phases made from aluminum nitrate as the preferred aluminum reagent exhibit narrow framework pore size distributions and average pore sizes that are independent of the surfactant size and packing parameter, in accord with a lathlike framework assembled from nanoparticles of regular size and connectivity. The high surface areas (~300−350 m^2/g) and pore volumes (~0.45−0.75 cm^3/g) provided by these mesostructured forms of γ-Al_2O_3 should be useful in materials and catalytic applications where the availability of surface Lewis acid sites and the dispersion of supported metal centers govern reactivity.

Introduction

Transition aluminas are intermediate phases formed in the process of thermally transforming aluminum hydroxides and oxyhydroxides into thermodynamically stable corundum or α-alumina. These high surface area aluminas have enormous commercial importance as adsorbents and catalyst components in many chemical processes, including the cracking and hydrocracking of petroleum,[1,2] the purification of gas oil fractions,[3,4] the steam reforming of hydrocarbon feedstocks to produce hydrogen,[5−7] and the control of automotive emissions[8,9] to name a few. The usefulness of transition aluminas can be traced to a favorable combination of textural properties (i.e., surface area, pore volume, and pore size distribution) and acid−base characteristics depending in part on the tetrahedral and octahedral site occupancy and on the degree of hydration and hydroxylation of the surface. At least seven different transition alumina phases have been claimed so far on the basis of ^{27}Al MAS NMR spectroscopy,[10,11] powder X-ray diffraction (XRD), and other scattering techniques.[1,12,13] Among these, γ-alumina is perhaps most extensively used in catalytic and adsorptive processes. γ-Alumina refers to the transition phase that has a spinel structure with a specific population of Al^{3+} defects in the tetrahedral (T_d) sites, as well as hydrogen ions in defect sites.[14] Conventional γ-alumina typically is prepared through the thermal dehydration of coarse particles of well-defined boehmite at a temperature above 400−450 °C.[1,12] Although amorphous aluminas can exhibit surface areas up to 800 m^2/g depending in part on the calcination temperature,[15] γ-aluminas typically have surface areas below 250 m^2/g and pore volumes less than

(1) Misra, C. *Industrial Alumina Chemicals*; ACS Monograph 184; American Chemical Society: Washington, DC, 1986.
(2) Knozinger, H.; Ratnasamy, P. *Catal. Rev.—Sci. Eng.* **1978**, *17*, 31.
(3) Prins, R.; De Beer, V. H. J.; Somorjai, G. A. *Catal. Rev.—Sci. Eng.* **1989**, *31*, 1.
(4) Prins, R. *Adv. Catal.* **2001**, *46*, 399.
(5) Maillet, T.; Barbier, J.; Gelin, P.; Praliaud, H.; Duprez, D. *J. Catal.* **2001**, *202*, 367.
(6) Velu, S.; Suzuki, K.; Okazaki, M.; Kapoor, M. P.; Osaki, T.; Ohashi, F. *J. Catal.* **2000**, *194*, 373.
(7) Bitter, J. H.; Seshan, K.; Lercher, J. A. *J. Catal.* **1998**, *176*, 93.
(8) Taylor, K. C. *Catal. Rev.—Sci. Eng.* **1993**, *35*, 457.
(9) Belton, D. N.; Taylor, K. C. *Curr. Opin. Solid State Mater. Sci.* **1999**, *4*, 97.
(10) John, C. S.; Alma, N. C. M.; Hays, G. R. *Appl. Catal.* **1983**, *6*, 341.
(11) Pecharroman, C.; Sobrados, I.; Iglesias, J. E.; Gonzalez-Carreno, T.; Sanz, J. *J. Phys. Chem. B* **1999**, *103*, 6160.
(12) Wefers, K.; Misra, C. *Oxides and Hydroxides of Aluminum*; Alcoa Laboratories: 1987.
(13) Zhou, R. S.; Snyder, R. L. *Acta Crystallogr.* **1991**, *47*, 617.
(14) Sohlberg, K.; Pantelides, S. T.; Pennycook, S. J. *J. Am. Chem. Soc.* **2001**, *123*, 26. Sohlberg, K.; Pennycook, S. J.; Pantelides, S. *J. Am. Chem. Soc.* **1999**, *121*, 7493. Krokidis, X.; Raybaud, P.; Gobichon, A. E.; Rebours, B.; Euzen, P.; Toulhoat, H. *J. Phys. Chem. B* **2001**, *105*, 5121.

10.1021/ja0208299 CCC: $22.00

0.50 cm^3/g, depending on the size and aggregation of the primary particles. Thus, the performance properties of γ-aluminas are decided in large part by their textural properties.

In view of the recent advancements realized for mesostructured silicas[16−24] as well as many other metal oxides,[25−27] one may anticipate similar improvements in the properties of γ-alumina through the formation of mesostructures. We have previously reported the preparation of mesostructured wormholelike aluminas (designated as MSU-X aluminas) with substantially improved surface area and porosity from aluminum *sec*-butoxide in the presence of electrically neutral block copolymer surfactants as the structure director.[28] Similar wormhole alumina mesostructures were also synthesized from aluminum alkoxides in the presence of anionic[29] and cationic surfactants.[30] A hexagonal alumina mesophase has been prepared through the hydrolysis of $Al(NO_3)_3$ using sodium dodecyl sulfate as the structure director,[31] but this composite was not stable to surfactant removal either by solvent extraction or by calcination, even when Y^{3+} was introduced as a dopant to stabilize the structure.[32] Also, a thermally stable disordered alumina mesostructure has been assembled from $AlCl_3$ and a nonionic triblock copolymer in ethanol solution.[33,34] This latter composition exhibited an exceptional surface area (~300 m^2/g), a broad pore size distribution, and a pore volume < 0.40 cm^3/g. In addition, a mesostructured alumina containing a transition alumina phase has been prepared from aluminum alkoxide and nonionic surfactants with amines as structure-modifying cosurfactants.[35]

All of the above mesostructured aluminas are comprised primarily of atomically disordered framework walls, as judged from the absence of well-expressed reflections in the wide-angle XRD patterns.[29,31] Further verification of atomic disorder in the framework walls has been provided by the presence of a substantial fraction of pentacoordinate aluminum centers, as determined by ^{27}Al MAS NMR spectroscopy.[28,29] Consequentially, these aluminas with amorphous framework walls have limited hydrolytic stability and lack the desired surface characteristics of a transition alumina phase for use as adsorbents and catalyst supports. For instance, they rapidly lose their mesostructured framework when suspended in water even at ambient temperature.

Recently, we reported the first mesostructured forms of alumina with crystalline framework walls.[36] These novel compositions, denoted MSU-γ, were assembled through the hydrolysis of aluminum alkoxides and aluminum salts in the presence of a nonionic triblock surfactant as the structure-directing porogen. The alkoxide precursors provided a scaffoldlike open framework structure, whereas aluminum salts afforded a framework with a porous lathlike (lamellar) structure. Somewhat larger surface areas, pore volumes, and pore sizes were observed for the scaffold frameworks than for the lathlike frameworks. However, from the standpoint of environmental and economical considerations, the lathlike frameworks made from aluminum salts should be more attractive candidates for potential applications in chemical catalysis and other materials applications.

In the present work we elucidate the stepwise reaction processes leading to the formation of mesostructured forms of γ-Al_2O_3 with lathlike framework morphologies from aluminum salts in the presence of both triblock $(EO)_x(PO)_y(EO)_x$ and diblock $RO(EO)_xH$ surfactants as the structure-directing porogens. In these formulations the EO, PO, and R units represent polymeric ethylene oxide, propylene oxide, and alkyl blocks, respectively. The crystalline walls of the resulting lathlike MSU-γ aluminas impart greatly improved hydrolytic stability in comparison to that of previously reported mesostructured aluminas with amorphous framework walls. These new mesostructures can be impregnated with catalyst precursors from aqueous solution, making them promising compositions for applications in chemical catalysis.

Experimental Section

Materials. An aluminum chlorohydrate solution containing the $Al_{13}O_4(OH)_{24}(H_2O)_{12}^{7+}$ oligocation (12.4 wt % Al) was provided by Reheis Company. Concentrated aqueous solutions containing 39 wt % $Al(NO_3)_3$ and 36 wt % $AlCl_3$ were prepared from reagent grade $Al(NO_3)_3 \cdot 9H_2O$ and $AlCl_3 \cdot 6H_2O$ purchased from Aldrich. Concentrated ammonium hydroxide (28 wt % NH_3) was purchased from Columbus Chemical Industries Inc. Nonionic triblock copolymer surfactants with principal compositions of $(EO)_{13}(PO)_{30}(EO)_{13}$ (Pluronic L64), $(EO)_{19}(PO)_{30}(EO)_{19}$ (Pluronic P65), $(EO)_{19}(PO)_{70}(EO)_{19}$ (Pluronic P84), and $(EO)_{19}(PO)_{70}(EO)_{19}$ (Pluronic P123) were obtained from BASF. Diblock surfactants of the type $RO(EO)_nH$ were provided by Union Carbide Corporation under the Tergitol trade name and denoted T-15-S-*n*, where R is a secondary alkyl group containing 11−15 carbon atoms and *n* is the number of ethylene oxide units in the polar block.

Synthesis Procedure. The following general procedure was used to prepare the mesostructured aluminas described in this study. A solution containing 0.10 mol of the desired aluminum precursor was mixed with the desired amount of surfactant in a blender for ~5 min. The resulting milky white mixture was aged in a reciprocal shaking bath at a temperature below 45 °C for ~36 h to form a clear sol. After this initial aging period, the sol was allowed to age an additional 6 h at a temperature between 45 and 90 °C. Ammonium hydroxide was slowly added under gentle stirring conditions to bring the total OH^-/

(15) Suh, D. J.; Park, T.-J. *Chem. Mater.* **1997**, *9*, 1903. Tanaka, K.; Imai, T.; Murakami, T.; Matsumoto, T.; Sugimoto, W.; Takasu, Y. *Chem. Lett.* **2002**, 110. Carnes, C. L.; Kapoor, P. N.; Klabunde, K. J.; Bonevich, J. *Chem. Mater.* **2002**, *14*, 2922.
(16) Kresge, C. T.; Leonowicz, M. E.; Roth, W. J.; Vartuli, J. C.; Beck, J. S. *Nature* **1992**, *359*, 710.
(17) Tanev, P. T.; Chibwe, M.; Pinnavaia, T. J. *Nature* **1994**, *368*, 321.
(18) Bagshaw, S. A.; Prouzet, E.; Pinnavaia, T. J. *Science* **1995**, *269*, 1242.
(19) Tanev, P. T.; Pinnavaia, T. J. *Science* **1996**, *271*, 1267.
(20) Corma, A. *Chem. Rev.* **1997**, *97*, 2373.
(21) Lu, Y. F.; Ganguli, R.; Drewien, C. A.; Anderson, M. T.; Brinker, C. J.; Gong, W. L.; Guo, Y. X.; Soyez, H.; Dunn, B.; Huang, M. H.; Zink, J. I. *Nature* **1997**, *389*, 364.
(22) Zhao, D. Y.; Feng, J. L.; Huo, Q. S.; Melosh, N.; Fredrickson, G. H.; Chmelka, B. F.; Stucky, G. D. *Science* **1998**, *279*, 548.
(23) Ying, J. Y.; Mehnert, C. P.; Wong, M. S. *Angew. Chem., Int. Ed.* **1999**, *38*, 56.
(24) Sayari, A.; Hamoudi, S.; Yang, Y.; Moudrakovski, I. L.; Ripmeester, J. R. *Chem. Mater.* **2000**, *12*, 3857.
(25) Antonelli, D. M.; Ying, J. Y. *Angew. Chem., Int. Ed. Engl.* **1995**, *34*, 2014.
(26) Antonelli, D. M.; Ying, J. Y. *Angew. Chem., Int. Ed. Engl.* **1996**, *35*, 426.
(27) Yang, P.; Zhao, D.; Margolese, D. I.; Chmelka, B. F.; Stucky, G. D. *Nature* **1998**, *396*, 152.
(28) Bagshaw, S. A.; Pinnavaia, T. J. *Angew. Chem., Int. Ed. Engl.* **1996**, *35*, 1102.
(29) Vaudry, F. J. P.; Khodabandeh, S.; Davis, M. E. *Chem. Mater.* **1996**, *8*, 1451.
(30) Cabrera, S.; El Haskouri, J.; Alamo, J.; Beltran, A.; Beltran, D.; Mendioroz, S.; Marcos, M. D.; Amoros, P. *Adv. Mater.* **1999**, *11*, 379.
(31) Yada, M.; Machida, M.; Kijima, T. *Chem. Commun.* **1996**, 769.
(32) Yada, M.; Ohya, M.; Machida, M.; Kijima, T. *Chem. Commun.* **1998**, 1941.
(33) Yang, P. D.; Zhao, D. Y.; Margolese, D. I.; Chmelka, B. F.; Stucky, G. D. *Nature* **1998**, *396*, 152.
(34) Yang, P. D.; Zhao, D. Y.; Margolese, D. I.; Chmelka, B. F.; Stucky, G. D. *Chem. Mater.* **1999**, *11*, 2813.
(35) Gonzalez-Pena, V.; Diaz, I.; Marquez-Alvarez, C.; Sastre, E.; Perez-Pariente, J. *Microporous Mesoporous Mater.* **2001**, *44−45*, 203.
(36) Zhang, Z. R.; Hicks, R. W.; Pauly, T. R.; Pinnavaia, T. J. *J. Am. Chem. Soc.* **2002**, *124*, 1592.

Al^{3+} molar ratio to a value between 3 and 3.6 and to achieve a pH value near 8.0. The solid gel was aged in a closed vessel for 6 h under ambient conditions to form an as-made mesostructured precursor, denoted MSU-X alumina. The as-made MSU-X was then subjected to hydrothermal conditions at 100 °C for 24 h to form a surfactant–intercalated boehmite mesophase, denoted MSU-S/B.

The surfactant and NH_4Cl byproduct were removed from the as-made MSU-X precursors by calcination at 550 °C, and the textural properties of these calcined mesostructures were compared with those of MSU-γ. CAUTION! As-made MSU-X mesostructures that have been assembled from $Al(NO_3)_3$ must not be calcined, as this will lead to an explosion of the thermodynamically unstable NH_4NO_3 byproduct.

The surfactant–boehmite mesostructures made from aluminum chlorohydrate and aluminum trichloride were converted to mesostructured MSU-γ phases with crystalline γ-Al_2O_3 walls by calcining the MSU-S/B mesophase at 325 °C for 3 h to sublime the NH_4Cl byproduct and then at 550 °C for 4 h to form the surfactant-free mesostructure. The MSU-S/B made from aluminum nitrate was first washed with distilled water to remove the NH_4NO_3 byproduct and then calcined at 500 °C to remove the surfactant. CAUTION! It is very important to remove the NH_4NO_3 byproduct through washing with water prior to converting the MSU-S/B surfactant–boehmite mesophase to MSU-γ to avoid an explosion of the ammonium nitrate under calcination conditions.

Physical Measurements. Powder XRD patterns were collected on a Rigaku Rotaflex diffractometer equipped with a rotating anode and Cu Kα radiation (λ = 0.154 nm). Counts were accumulated every 0.02° (2 Å) at a scan speed of 2° (2 Å)/min. N_2 adsorption–desorption isotherms were obtained at −196 °C on a Micromeritics ASAP 2010 Sorptometer using a static adsorption procedure. Samples were degassed at 150 °C and 10^{-6} Torr overnight prior to analysis. BET surface areas were calculated from the linear part of the BET plot. Pore size distributions were calculated from the adsorption isotherms by the Barrett–Joyner–Halenda (BJH) model, and the total pore volumes were estimated from the N_2 uptake at P/P_0 = 0.995. Transmission electron microscopic (TEM) images and electron diffraction (ED) patterns of selected fields were obtained on a JEOL 100CX microscope equipped with a CeB_6 filament and an accelerating voltage of 120 kV. Sample grids were prepared by sonicating powdered samples in ethanol for 20 min and evaporating one drop of the suspension onto a carbon-coated, holey film supported on a 3 mm, 300-mesh copper grid.

Results

Three aluminum salts were examined as reagents for the synthesis of MSU-γ aluminas with lathlike framework morphologies, namely, $AlCl_3 \cdot 6H_2O$, $Al(NO_3)_3 \cdot 9H_2O$, and aluminum chlorohydrate. The latter chloride salt, which is supplied in the form of an aqueous solution under the trade name Aluminum Chlorohydrol, contains primarily the Al_{13} oligocation $[Al_{13}O_4(OH)_{24}(H_2O)_{12}]^{7+}$.[37–39] Regardless of which salt is selected as a precursor, the overall synthesis procedure involves three discrete chemical reactions, each of which leads to a compositionally distinct mesostructure. In the first reaction step, the salt is hydrolyzed with NH_4OH at a temperature in the range 45–90 °C and at pH ~8.0 in the presence of a nonionic ethylene oxide surfactant. This step results in the formation of a mesostructure, denoted MSU-X alumina, with a wormhole to spongelike pore structure.

Evidence for the formation of wormhole mesostructures with amorphous walls in the first assembly step is provided by the XRD patterns shown in Figure 1 for the mesostructures formed

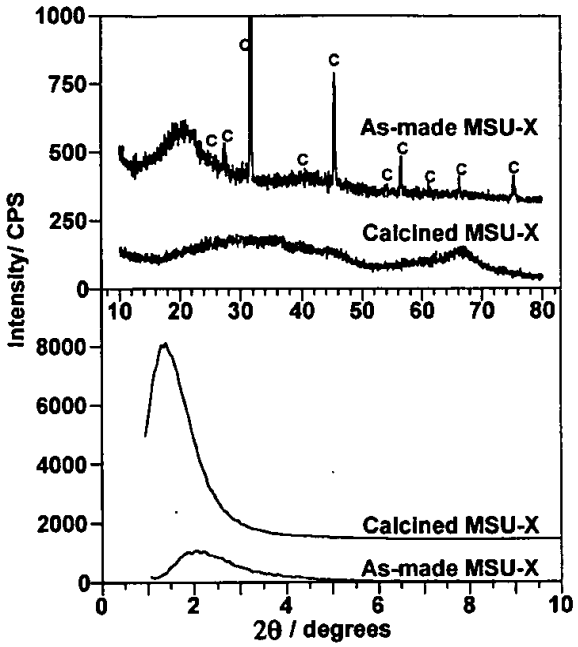

Figure 1. XRD patterns in the 2 Å ranges 1–10° (lower patterns) and 10–80° (upper patterns) for as-made (70 °C) and calcined (550 °C) MSU-X mesostructures assembled from Al_{13} oligocations and the triblock surfactant $(EO)_{19}(PO)_{43}(EO)_1$ (Pluronic P84). The sharp reflections labeled "C" in the pattern of the as-made mesostructure arise from the NH_4Cl byproduct.

from Al_{13} oligocations in the presence of Pluronic P84 as the surfactant. Both the as-made and calcined mesostructures exhibited a broad reflection in the small angle region near 2 Å = 2.0°, which is characteristic of a wormhole or spongelike framework.[18,19,28–30,40] The wide-angle regions of the pattern between 10° and 80° for the as-made mesostructure contain narrow diffraction lines corresponding to the NH_4Cl byproduct and a very diffuse reflection near 2 Å = 20° that we attribute to the correlation distance between aggregated surfactant molecules in the framework pores. The absence of diffraction lines characteristic of an ordered oxide phase is in accord with a mesostructure with amorphous framework walls. Equivalent XRD patterns were observed for the as-made MSU-X mesostructure assembled from $AlCl_3 \cdot 6H_2O$ and $Al(NO_3)_3 \cdot 9H_2O$, except that in the case of the latter reagent the narrow lines in the wide-angle XRD pattern corresponded to NH_4NO_3 as a reaction byproduct.

Very diffuse, weak reflections (cf., Figure 1) are observed in the wide-angle region of the XRD patterns of MSU-X aluminas calcined at 500–550 °C. (Caution! See Experimental Section regarding potential explosion hazard.) Although diffuse lines near 2 Å values of 46 and 66° suggest the onset of some atomic ordering, the framework walls are substantially amorphous. The TEM images shown in Figure 2 for the calcined MSU-X aluminas assembled from Al_{13} oligocations, $AlCl_3$, and $Al(NO_3)_3$ verify the presence of a wormhole to spongelike framework with amorphous walls. Analogous alumina mesostructures have been assembled previously from aluminum alkoxides[28,41] or aluminum chloride[33,34] in the presence of nonionic surfactants, as well as from ionic surfactants.[30]

(37) Fitzgerald, J. J.; Johnson, L. E. *J. Magn. Reson.* **1989**, *84*, 121.
(38) Akitt, J. W.; Elders, J. M. *J. Chem. Soc., Dalton Trans.* **1988**, 1347.
(39) Roswell, J.; Nazar, L. F. *J. Am. Chem. Soc.* **2000**, *122*, 3777.
(40) Tanev, P. T.; Pinnavaia, T. J. *Science* **1995**, *267*, 865.
(41) Deng, W.; Bodart, P.; Pruski, M.; Shanks, B. H. *Microporous Mesoporous Mater.* **2002**, *52*, 169.

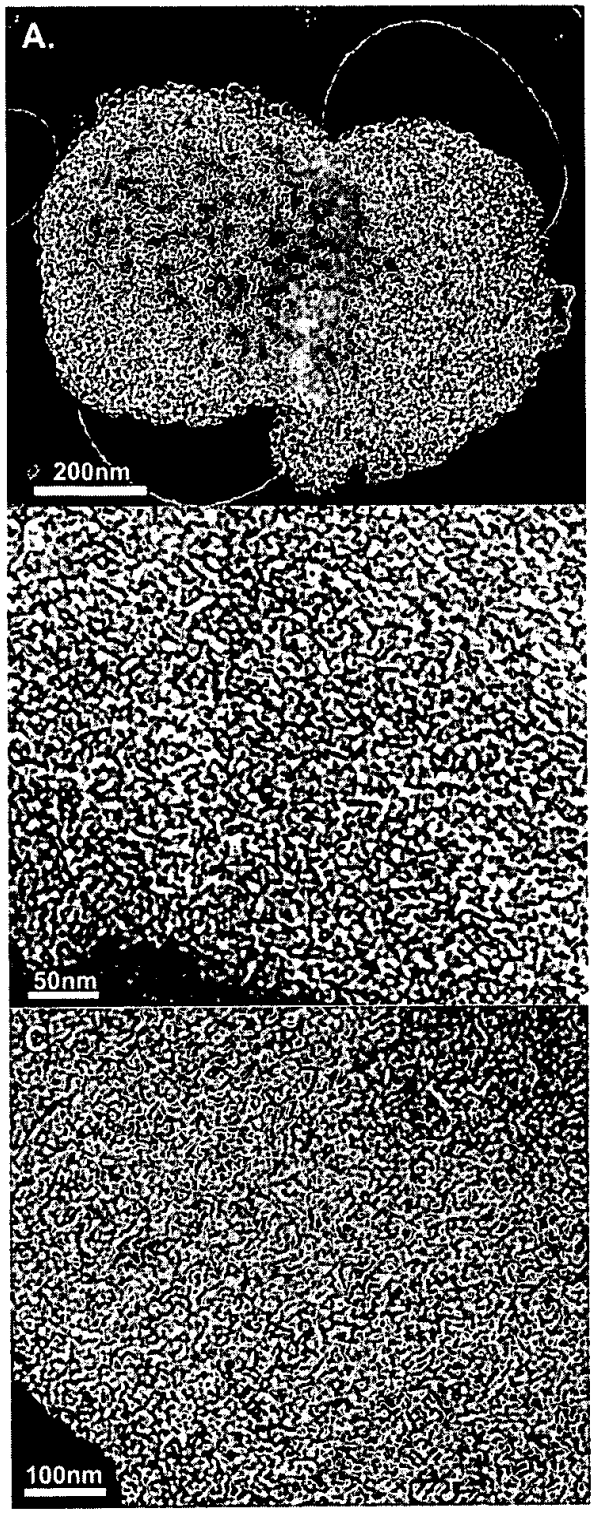

Figure 2. TEM images of MSU-X aluminas with wormhole framework structures and amorphous framework walls; the mesostructures were assembled at 70 °C from Plúronic P84 as the structure directing porogen and (A) Al_{13} oligocations, (B) $Al(NO_3)_3$, and (C) $AlCl_3$ as the aluminum reagent.

The textural parameters shown in Table 1 for representative MSU-X aluminas verify that these wormhole mesostructures form through a supramolecular assembly mechanism. In the case

Table 1. Synthesis Parameters and Structural Properties of Calcined MSU-X Aluminas Assembled from Aluminum Salts and Pluronic $(EO)_n(PO)_m(EO)_n$ Surfactants[a]

aluminum precursor	surf	Al/surf/OH^- molar ratio	T (°C)	S_{BET} (m^2/g)	pore size[b] (nm)	pore vol[c] (cm^3/g)	d_{100} (nm)
Al_{13}[d]	P84	1:0.011:3.0	45	249	9.6	0.55	>10
Al_{13}	P84	1:0.011:3.0	60	343	7.4	0.81	7.2
Al_{13}	P84	1:0.011:3.0	70	322	7.0	0.75	6.4
Al_{13}	P84	1:0.011:3.0	90	367	5.6	0.51	5.6
Al_{13}	P65	1:0.014:3.0	70	319	6.1	0.53	5.5
Al_{13}	L64	1:0.016:3.0	70	310	5.1	0.57	5.1
$AlCl_3$	P84	1:0.015:3.6	70	308	6.8	0.66	9.8
$Al(NO_3)_3$	P84	1:0.015:3.6	70	330	4.0	0.65	5.4

[a] Formulas for the triblock Pluronic surfactants are given in the text. [b] BJH pore sizes were determined from N_2 desorption isotherms. [c] Pore volumes were determined from the N_2 uptake at $P/P_0 = 0.995$. [d] Al_{13} denotes the chloride salt of the $Al_{13}O_4(OH)_{24}(H_2O)_{12}^{7+}$ cation.

of P84 as the structure-directing surfactant, both the pore size and the pore–pore correlation distance (d_{001}) decrease with increasing assembly temperature over the range 45–90 °C. This is consistent with the incorporation of less surfactant into the mesostructure as the assembly temperature moves through the cloud point of the surfactant (75 °C). Also, the framework pore size increases with increasing surfactant size, as expected for a supramolecular assembly pathway.

Having identified the as-made and calcined MSU-X mesostructures formed in the first reaction step as being the products of a supramolecular assembly process with the surfactant acting as a structure-directing porogen, we next describe the products formed in the second and third steps in the reaction sequence leading to the formation of MSU-γ aluminas. The second reaction step transforms the as-made MSU-X intermediate into a surfactant–boehmite mesophase, denoted MSU-S/B, through hydrothermal treatment at 100 °C. The third reaction converts the boehmitic MSU-S/B mesophase to the desired MSU-γ mesostructure through calcination at 500–550 °C. (CAUTION! See Experimental Section regarding potential explosion hazard.) This final step in the synthesis of MSU-γ results in the removal of the surfactant phase and the conversion of the boehmitic mesophase into a MSU-γ mesostructure with walls made of γ-Al_2O_3.

XRD patterns for a typical MSU-S/B surfactant–boehmite mesophase and the corresponding MSU-γ alumina formed through calcination are shown in Figure 3. The MSU-X precursor to these two phases was assembled from aluminum nitrate and a P84 surfactant. The as-made MSU-X precursor was washed free of the NH_4NO_3 byproduct before being converted to MSU-S/B and MSU-γ. Both mesostructures exhibit a single reflection in the low 2 Å region below 2°. The broad reflections for MSU-S/B in the 2 Å region between 10° and 80° correspond to boehmite (JCPDS Card 21-1307), whereas those for MSU-γ are in accord with γ-alumina (JCPDS Card 10-0425). Equivalent XRD patterns were observed for the MSU-S/B and MSU-γ phases derived from Al_{13} oligocations and aluminum chloride as the aluminum reagent.

A TEM image for a typical mesophase formed through the hydrothermal treatment (100 °C) of a MSU-X precursor is shown in Figure 4A. In this case the precursor was assembled from Al_{13} oligomers and P84 surfactants. Note that the wormhole to spongelike framework morphology characteristic of the precursor (cf., Figure 2A) has been replaced by thin, lathlike nanolayers of the boehmitic MSU-S/B mesophase. This

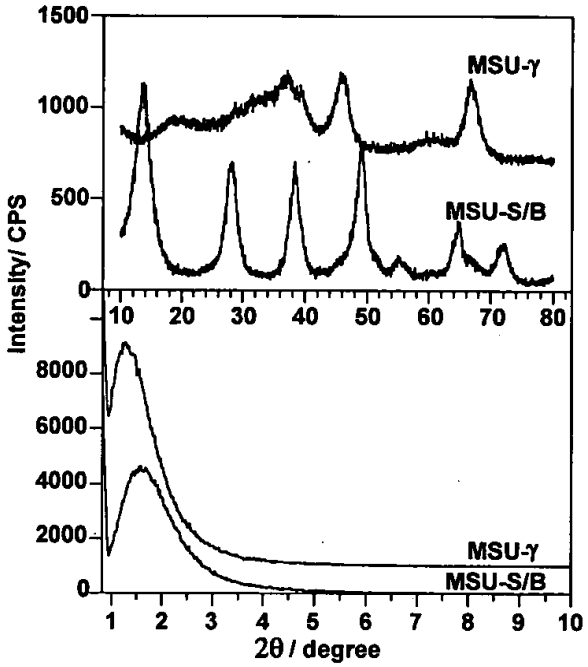

Figure 3. XRD patterns in the 2 Å regions 1−10° (lower pattern) and 10−80° (upper pattern) for a mesostructured MSU-S/B surfactant−boehmite mesophase assembled at 70 °C from $Al(NO_3)_3$ and Pluronic P84, and the corresponding MSU-γ mesostructure formed by calcining the MSU-S/B intermediate at 500 °C.

signifies that the transformation is atopochemical. Slit-shaped mesopores are present between the laths, and the laths propagate to form flakelike particles that adopt different relative orientations. The conversion of the intermediate MSU-S/B mesophase to a surfactant-free MSU-γ through calcination at 500−550 °C occurs with retention of the lathlike framework morphology, as shown by the TEM images in Figure 4B and C. There is no doubt that the lathlike framework is made of γ-Al_2O_3 walls, as judged from the electron diffraction pattern shown in Figure 5A. This pattern, which was obtained from mesostructured particles with the morphology shown in Figure 5B, contains the three strongest reflections of γ-Al_2O_3.

It is also possible to obtain MSU-S/B and MSU-γ mesostructures structurally equivalent to those represented in Figures 4 and 5 by replacing the structure-directing Pluronic P84 surfactant $(EO)_{19}(PO)_{43}(EO)_{19}$ with other triblock surfactants, including Pluronic P123, P65, and L64 with molecular structures corresponding to $(EO)_{20}(PO)_{70}(EO)_{20}$, $(EO)_{19}(PO)_{30}(EO)_{19}$, and $(EO)_{13}(PO)_{30}(EO)_{13}$, respectively. In addition, diblock Tergitol surfactants of the type $RO(EO)_xH$, denoted T15-S-*n*, where *n* is the number of ethylene oxide units in the hydrophilic block and R is a secondary alkyl containing 11−15 carbon atoms, were found to be effective in forming mesostructured MSU-X, MSU-S/B, and MSU-γ phases under analogous stepwise reaction sequences.

The textural properties of representative MSU-γ aluminas, as determined from N_2 adsorption−desorption isotherms, are provided in Table 2. Included in the table are the synthesis parameters used to prepare the MSU-X precursors in the initial assembly step. Typical isotherm shapes are presented in Figure 6. The MSU-γ mesostructures derived from $AlCl_3$ and $Al(NO_3)_3$ as reagents in the initial assembly reaction characteristically

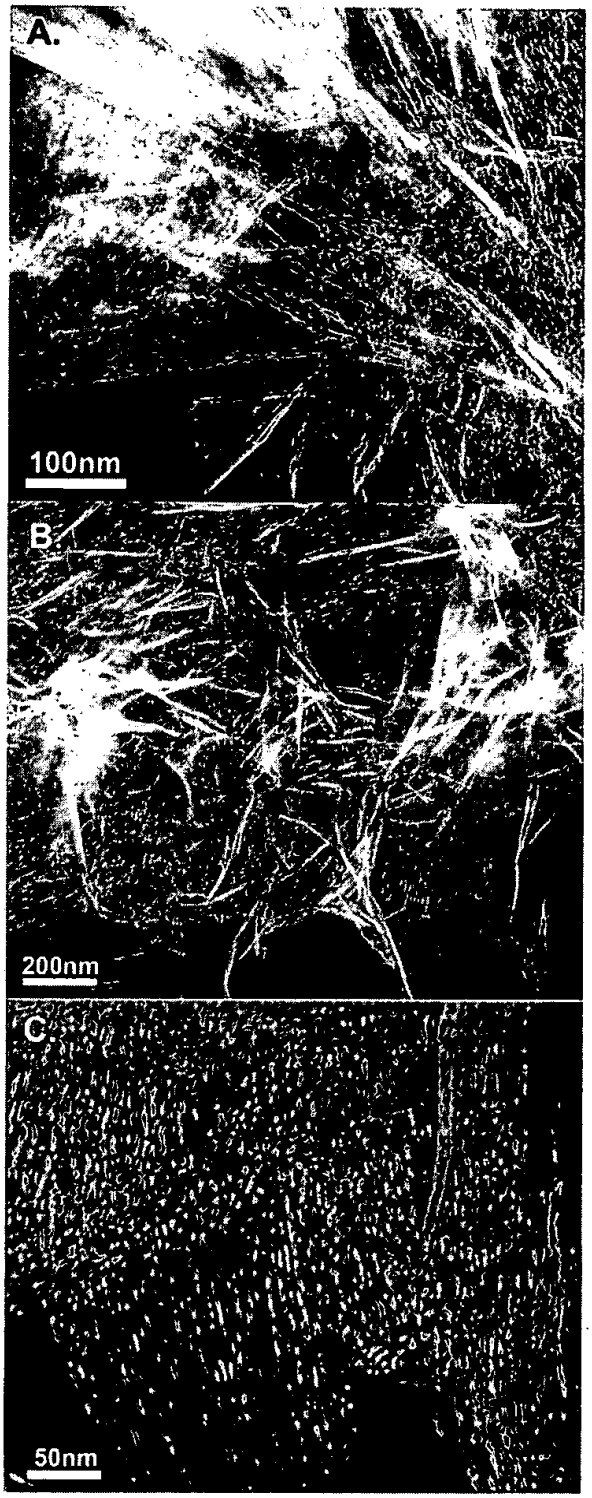

Figure 4. TEM images of (A) surfactant−boehmite mesophase (MSU-S/B) made at 70 °C from Al_{13} oligocations and Pluronic P84 surfactant, and (B and C) the corresponding MSU-γ phase with crystalline γ-Al_2O_3 walls formed through calcination of the MSU-S/B mesophase at 550 °C for 4 h.

exhibit type IV isotherms with little or no additional uptake at high partial pressures. However, the analogous mesostructures derived from Al_{13} oligocations show a hysteresis at high partial pressure, which is consistent with the much broader pore size

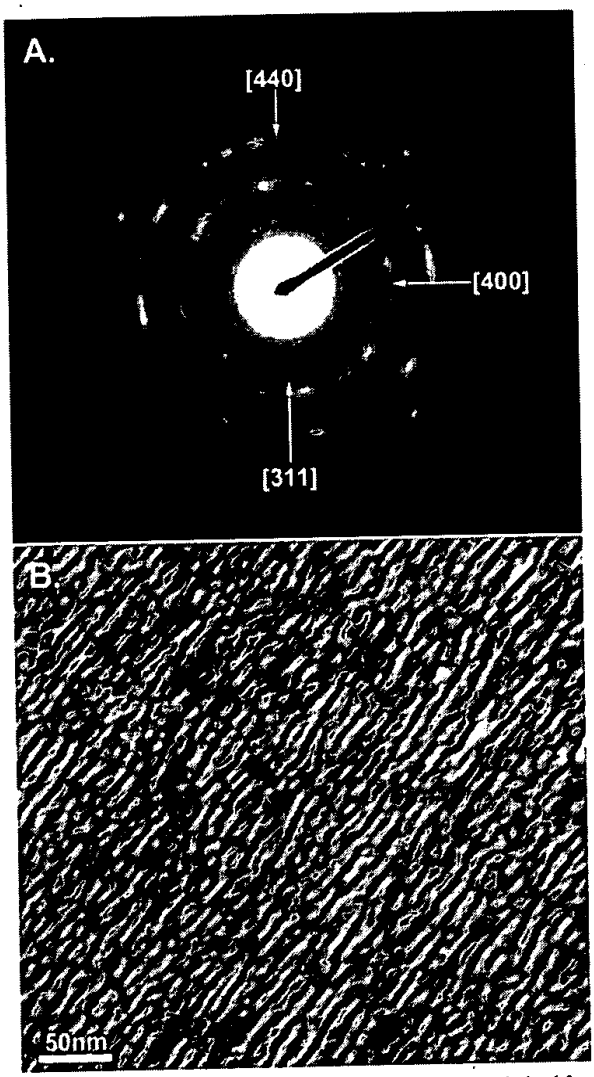

Figure 5. (A) Electron diffraction pattern of MSU-γ aluminas derived from Al_{13} oligocations and Pluronic P84 surfactant at an assembly temperature of 70 °C and (B) the TEM image of the framework mesostructure giving rise to the diffraction pattern.

distribution found for these derivatives (cf., inset to Figure 6). Also, it is noteworthy that the average pore size for the MSU-γ mesostructures derived from the chloride salts of Al_{13} oligocations and hydrated Al^{3+} cations can be substantially larger than the average pore−pore correlation distance obtained from the d_{001} X-ray spacing (see Table 2). The nitrate salt, however, affords MSU-γ mesostructures with average BJH pore sizes that are consistently smaller than the pore−pore correlation distance, though the pore sizes are nearly independent of the size of the surfactant used to assemble the initial MSU-X precursor.

Discussion

Figure 7 summarizes the sequence of reaction steps leading to the formation of the mesostructured γ-aluminas prepared in this work. The reaction conditions indicated in the figure are preferred, in general. Mesostructured MSU-X type aluminas with a wormhole framework are formed in the first reaction step through a supramolecular assembly process. The calcined forms of these aluminas are structurally and compositionally equivalent to previously reported mesostructured aluminas.[28−30,34,35] Although the extremely diffuse reflections observed in the wide-angle regions of the diffraction patterns obtained in the present work (cf., Figure 1), as well as in earlier studies,[35] are suggestive of the onset of γ-alumina formation, the walls of the calcined mesostructures are essentially amorphous. Although MSU-X mesostructures can be calcined in air at temperatures up to 800 °C for several hours with retention of structure,[41] particularly when doped with rare earth elements,[42] the mesostructured framework is very sensitive to moisture. The low-angle diffraction peak is rapidly lost when the calcined mesostructure is suspended in water or when allowed to age under ambient conditions for several months. Thus, the potential advantages of the regular mesoporosity, high surface areas, and pore volumes offered by these aluminas, as well as by all previously reported aluminas with amorphous framework walls, for materials applications and chemical catalysis are severely compromised.

The MSU-X aluminas generated in the first hydrolysis step, however, are novel precursors for transformation to mesostructured MSU-S/B surfactant−boehmite mesophases that can be further transformed upon calcination into the desired mesostructured MSU-γ aluminas with framework walls made of lathlike γ-Al_2O_3 nanoparticles (see the second and third steps Figure 7). To our knowledge, the transformation of a preassembled mesostructure made by a supramolecular process into a new framework structure made of crystalline nanoparticles has not been recognized previously. Moreover, unlike previously reported mesostructured aluminas with amorphous framework walls, the crystalline framework of MSU-γ alumina is stable in aqueous suspension and, as will be shown in future work, can be readily impregnated with transition metal catalyst precursors without the loss of framework porosity, surface area, or pore volume. Whereas conventional γ-aluminas have surface areas and pore volumes of <250 m^2/g and <0.50 cm^3/g, respectively, the mesostructured forms reported in the present work exhibit substantially higher surface areas and pore volumes that are typically in the respective ranges 300−350 m^2/g and 0.45−0.75 cm^3/g. Thus, the improved textural porosities of mesostructured MSU-γ aluminas should be advantageous in materials applications such as sensing[45] and in heterogeneous catalysis where the availability of surface Lewis acid sites and the dispersion of supported metal centers on the alumina govern reactivity. It should be noted that although the magnitudes of the porosity parameters for MSU-γ aluminas are lower than those normally observed for mesostructured silicas,[16−19,22,40,46] the thick framework walls (see TEM images in Figures 4C and 5B), together with the high density of γ-Al_2O_3 (~3.3 g/cm^3) in comparison to amorphous silica (~2.2 g/cm^3), account for the comparatively lower surface areas.[36]

There are several mechanistic aspects of the stepwise reaction sequence shown in Figure 7 that are particularly notable. That the formation of the mesostructured MSU-X aluminas in the initial reaction step occurs through a supramolecular assembly

(42) Zhang, W.; Pinnavaia, T. J. *Chem. Commun.* **1998**, 1185.
(43) Pauly, T. R.; Liu, Y.; Pinnavaia, T. J.; Billinge, S. J. L.; Rieker, T. P. *J. Am. Chem. Soc.* **1999**, *121*, 8835.
(44) Liu, Y. C.; Chen, S. H.; Huang, J. S. *Macromolecules* **1998**, *31*, 6226.
(45) Dickey, E. C.; Varghese, O. K.; Ong, K. G.; Gong, D.; Paulose, M.; Grimes, C. A. *Sensors* **2002**, *2*, 91.
(46) Kruk, M.; Jaroniec, M.; Guan, S.; Inagaki, S. *J. Phys. Chem. B* **2001**, *105*, 681.

Table 2. Textural Properties of Crystalline MSU-γ Aluminas Derived from Amorphous MSU-X Precursors[a]

amorphous MSU-X assembly conditions				crystalline MSU-γ textural properties			
aluminum reagent	surfactant[b]	Al^{3+}/surf/OH^- molar ratio	T (°C)	S_{BET} (m^2/g)	pore size[c] (nm)	pore vol[d] (cm^3/g)	d_{001} (nm)
Al_{13}	P84	1:0.011:3.0	70	299	8.0	0.73	6.6
Al_{13}	P65	1:0.014:3.0	70	309	5.9	0.73	5.8
Al_{13}	L64	1:0.016:3.0	70	307	5.8	0.53	5.1
$AlCl_3$	P84	1:0.015:3.6	70	311	8.2	0.69	6.3
$Al(NO_3)_3$	P123	1:0.011:3.6	40	336	3.9	0.56	6.4
$Al(NO_3)_3$	P84	1:0.015:3.6	70	325	4.0	0.50	6.7
$Al(NO_3)_3$	P65	1:0.019:3.6	70	313	3.9	0.44	5.3
$Al(NO_3)_3$	L64	1:0.022:3.6	50	346	3.7	0.46	4.9
$Al(NO_3)_3$	T15-S-30	1:0.042:3.6	70	297	4.0	0.43	6.0
$Al(NO_3)_3$	T15-S-20	1:0.058:3.6	70	302	4.1	0.47	6.0
$Al(NO_3)_3$	T15-S-15	1:0.073:3.6	70	320	4.2	0.47	5.3
$Al(NO_3)_3$	T15-S-12	1:0.085:3.6	70	254	4.1	0.39	5.5

[a] The calcination temperature was 500 °C except for the first four entries in the table where it was 550 °C. [b] The surfactant formulas are provided in the text. [c] BJH pore size. [d] Nitrogen pore volumes at $P/P_0 = 0.995$.

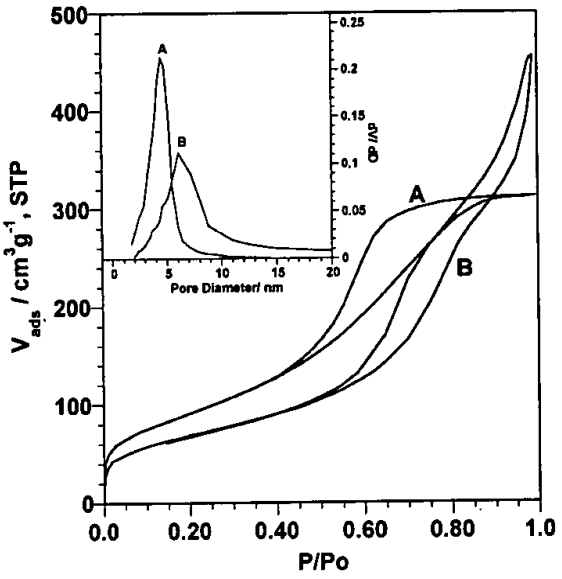

Figure 6. N_2 adsorption–desorption isotherms and BJH pore size distributions (inset) for MSU-γ aluminas derived from Pluronic P84 surfactant and (A) $Al(NO_3)_3$ and (B) Al_{13} oligocations as the aluminum reagent. The assembly temperature in each case was 70 °C.

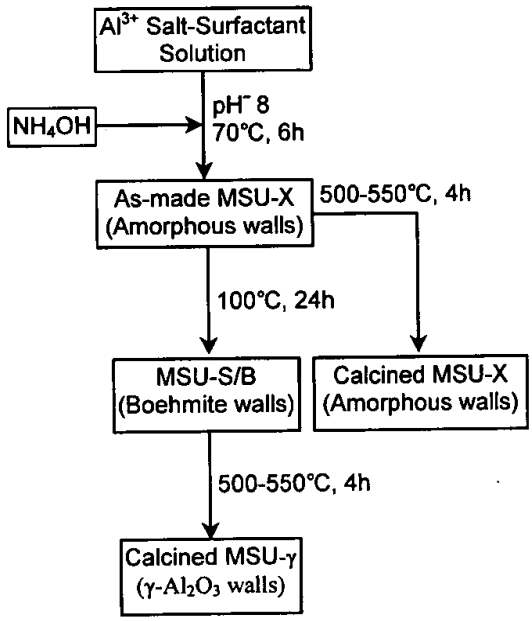

Figure 7. Reaction sequence used for the consecutive formation of MSU-X aluminas with amorphous framework walls, MSU-S/B surfactant–boehmite mesophase with boehmite framework walls, and MSU-γ aluminas with framework walls made of γ-Al_2O_3 nanoparticles.

process is evidenced by the formation of a wormhole framework structure with pore sizes that depend on the size of the structure-directing surfactant and the assembly temperature (cf., Figure 2 and Table 1). The pore–pore correlation distances obtained from the d_{001} X-ray reflections are comparable to the average BJH pore sizes derived from the nitrogen adsorption isotherms, suggesting that the BJH model, which is based on cylindrical pores rather than slit-shaped pores,[47] may overestimate to some extent the framework pore size. The pore sizes estimated from the TEM images, however, are commensurate with the BJH pore sizes, so the model does not grossly overestimate the pore sizes.

The transformation of the amorphous framework walls of MSU-X into the boehmitic walls of the MSU-S/B intermediate is clearly atopochemical, as evidenced by a dramatic change in framework structure from one that is wormholelike to one that is lamellar or lathlike (e.g., compare TEM images in Figures 2 and 4). However, the subsequent thermal transformation of the boehmitic AlO(OH) walls of the MSU-S/B mesophase to MSU-γ alumina does occur with retention of framework morphology (e.g., see TEM images in Figure 4). We have not yet been able to remove the surfactant from the MSU-S/B intermediate, thus precluding the direct characterization of the framework pore structure. However, in view of the topochemical nature of the MSU-S/B to MSU-γ transformation, we infer that the textural properties of the former mesostructure parallel those of the latter. Thus, we can deduce some of the factors that determine the porosity observed for the MSU-γ mesostructures.

The nonionic surfactants that are contained in the framework and interparticle pores of the initially assembled MSU-X mesostructures undoubtedly play an important role in the transformation of the initially amorphous alumina walls into assemblies of boehmite nanoparticles in the second step of the reaction sequence. Evidence suggesting that the counteranions of the initial aluminum reagent also contribute to the porosity

(47) Gregg, S. J.; Sing, K. S. W. *Adsorption, Surface Area and Porosity*, 2nd ed.; Academic Press: London, 1982.

of MSU-S/B precursors is provided by the very different shapes of the nitrogen isotherms observed for the final MSU-γ reaction products. The mesostructures made from Al_{13} oligocations typically exhibit a complex isotherm with hysteresis at high partial pressures and a relatively broad pore size distribution (see Figure 6), whereas those made from $AlCl_3$ and $Al(NO_3)_3$ exhibit classic type IV isotherms[47] and a comparatively narrow pore size distribution. Since aqueous Al^{3+} ions are rapidly converted to Al_{13} and other oligocations upon basic hydrolysis,[37-39] one might have expected the porosity to be independent of the choice of the aluminum precursor. However, the hydrolysis of Al_{13} oligocations requires the addition of far less NH_4OH ($OH^-/Al^{3+} \sim 0.5$) in comparison to aqueous Al^{3+} ions ($OH^-/Al^{3+} \sim 3.0-3.6$) to form the hydrated alumina walls of MSU-X mesostructures. Thus, the boehmitic MSU-S/B aluminas made from aqueous aluminum cations are assembled in the presence of 6.0−7.2 times more NH_4Cl or $NH_4(NO_3)_3$ in comparison to those made from Al_{13} oligocations.

The higher ionic strength provided by $AlCl_3$ and $Al(NO_3)_3$ as starting reagents affords more monolithic particles of MSU-S/B. Thus, well-expressed type IV isotherms with narrow pore size distributions but no high partial pressure hysteresis are observed for the MSU-γ aluminas made from $AlCl_3$ and $Al(NO_3)_3$, as expected for monolithic assemblies that lack interparticle textural porosity. In contrast, the thin, lamellar, and highly textured particles of MSU-γ made from Al_{13} oligomers exhibit complex isotherms and broad pore size distributions (cf., Figure 6), consistent with a large fraction of the porosity arising from inter- and intraparticle voids.

Ionic strength differences, however, cannot explain the fact that the average pore size of the MSU-γ mesostructures made from the chloride salts of both Al_{13} oligocations and aqueous Al^{3+} ions often exceeds the average pore−pore correlation distance obtained by XRD (cf., Table 2). This behavior suggests that a substantial fraction of the total porosity of the MSU-γ compositions made from chloride salts of aluminum does not arise exclusively from a regularly mesostructured nanoparticle framework. Instead, some nonframework mesoporosity (most likely arising from both inter- and intraparticle textural porosity) also is present that does not contribute to the observed pore−pore correlation distance. In contrast, the MSU-γ compositions made from the nitrate salt consistently exhibit a correlation distance that is larger than the pore size, as expected for well-expressed mesostructures. That the MSU-γ mesostructures derived from the chloride salts are more disordered than those made from $Al(NO_3)_3$ may be related to the fact that MSU-S/B intermediates incorporate 0.80−3.4 wt % chloride ion but little or no nitrate ion. This chloride cannot be removed by washing, presumably because it is incorporated into the framework walls. As discussed below, the incorporation of chloride ions into the framework may affect the pore forming mechanism. Thus, $Al(NO_3)_3$ is the preferred reagent for the synthesis of mesostructured MSU-γ alumina.

One additional final feature of the synthetic chemistry leading to γ-Al_2O_3 formation is especially important. For the well-ordered MSU-γ aluminas made from $Al(NO_3)_3$, the pore sizes of the resulting mesostructures are independent of the surfactant size or packing parameter (see Table 2). This signifies that, regardless of the surfactant size, only a limited amount of the surfactant is capable of functioning as a porogen in the conversion of assembled MSU-S/B nanoparticles into the corresponding MSU-γ alumina. Because MSU-S/B and -γ aluminas have topochemically related framework structures and the conversion of boehmite to γ-Al_2O_3 (>400 °C) occurs at a temperature higher than the decomposition or vaporization temperature of the surfactant, the pore structure of MSU-γ is predetermined by the assembly of nanoparticles in the boehmitic MSU-S/B mesophase. Thus, the amount of surfactant that is intercalated between the alumina laths is determined by the thickness of the laths and the degree to which the laths fuse and cross-link together in forming a mesostructure. The latter process is controlled in part by the adsorption of surfactant on the nanoparticle surfaces. As can be seen from the TEM images provided in Figures 4C and 5B, the framework walls are not truly lamellar but are comprised of lathlike slabs that split, merge, and cross-link to form the slitlike pores. Thus, the framework pore structure of these MSU-γ aluminas is a consequence of fundamental particle assembly, as opposed to a supramolecular assembly process in which an inorganic framework is formed around micellar surfactant domains whose size is determined by surfactant packing parameters. A particle assembly mechanism also may explain why factors such as differences in ionic strength and the incorporation of chloride ions into the framework can induce disorder sufficient to cause the average pore size to be larger than the correlation distance between the ordered pores.

Zhu et al.[48] have recently reported the synthesis of γ-Al_2O_3 fibers through the use of nonionic Tergitol surfactants to control the crystal growth of a boehmite precursor formed from sodium aluminate solution. The PEO surfactant to aluminum molar ratios used to form the fibers was >0.47, far higher than the 0.04−0.09 ratios used in the assembly processes reported in the present work. Although the fibrous γ-alumina was not mesostructured, the low-contact aggregation of the fibers gave rise to very high textural porosity (1.2−2.0 cm^3/g). Surfactant-induced fiber formation was attributed to hydrogen bonding interactions between the PEO headgroups of the surfactant and the boehmite surfaces. Similar hydrogen bonding interactions are likely to operate in the surfactant-directed assembly of boehmite nanoparticles under our reaction conditions. Additional studies of this aspect of the pore forming process will be needed, however, to more fully elucidate the surfactant−alumina interactions that control the thickness of the laths and the degree to which they merge, cross-link, and assemble to form framework mesopores.

Acknowledgment. The support of this research by the National Science Foundation through Grant CHE-9903706 is gratefully acknowledged. *Corresponding author. Fax: (517) 432-1225. E-mail: Pinnavai@cem.msu.edu.

JA0208299

(48) Zhu, H. Y.; Riches, J. D.; Barry, J. C. *Chem. Mater.* **2002**, *14*, 2086.